Hydroxyapatite Nanoparticles for Acidic Mine Waters Remediation

CLAUDIA MARIA SIMONESCU[1]*, DANIELA CRISTINA CULITA[2], VIRGIL MARINESCU[3], CHRISTU TARDEI[3], DORINEL TALPEANU[3]
[1]University Politehnica of Bucharest, Faculty of Applied Chemistry and Materials Science, Department of Analytical Chemistry and Environmental Engineering, 1-7 Polizu Str., 011061 Bucharest, Romania
[2]Ilie Murgulescu Institute of Physical Chemistry, 202 Splaiul Independentei, 060021, Bucharest, Romania
[3]National Institute for R&D in Electrical Engineering ICPE-CA, Department of Advanced Materials, 313 Splaiul Unirii Str., 030138 Bucharest, Romania

Mining activities have a high negative impact on the environment and on human health. Environmental impacts can result in contamination of surface water, groundwater, soil and air. Large volumes of wastewater produced by mining activities have to be remediated before being discharged into the environment. Due to the complex composition of wastewater coming from the mining industry and because their negative impacts, numerous remediation techniques have been applied. Adsorption is one of the most extensively used ways to remediate mining wastewater as a consequence of its low cost, easiness to be performed, and also due to the wide variety of materials (natural and synthetic) that can be use as adsorbents. Hydroxyapatite (HAP, $Ca_{10}(PO_4)_6(OH)_2$), a naturally occurring form of calcium phosphate has a good capacity to remove heavy metal ions from aqueous solutions due to its excellent properties. By preparing hydroxyapatite using different synthesis methods, its properties can be manipulated in order to increase the adsorption properties and reactivity. Herein, we reported synthesis of hydroxyapatite (HAP) samples using different synthesis conditions to establish the effect of synthesis conditions onto HAP properties. The HAP samples prepared have been characterized by the use of X-ray diffraction, FT-IR spectroscopy, specific surface measurements, Scanning Electron Microscopy (SEM). The stoichiometric compounds with high degree of crystallinity, low average particle diameter values, and low specific surface have been prepared by the solid state reaction and high calcination temepratures. The addition of surfactant (dispersant) has resulted in an increase in the specific surface area, which will result in an increase in the retention capacity of heavy metal ions in wastewater. The adsorbents prepared were used to remediate mine water. Results showed that non-calcinated HAP samples have a higher heavy metals adsorption capacity compared to HAP samples calcinated at 600 °C and 900 °C. The HAP samples prepared in presence of surfactant exhibit a higher heavy metals adsorption capacity than samples prepared in absence of surfactant. The values of the retention capacity differ depending on the nature of the metal ion: $Q_{Mn(II)} > Q_{Fe(III)} > Q_{Zn(II)} > Q_{Pb(II)} > Q_{Ni(II)}$. *A change in the pH of mine water from 2.6 to 5.5 has occur that means that the metal ion retention mechanism goes through chemical reactions. The metal ions retention capacity suggests application of hydroxyapatite for remediation of mining wastewater.*

Keywords: hydroxyapatite synthesis, solid state reaction, adsorption, mine water remediation, surfactant, calcination

Pollution of surface waters and groundwater caused by heavy metal ions, as well as organic chemicals (halogenated hydrocarbons, benzene, toluene, pesticides) and other inorganic species (nitrates, phosphates) is a major environmental problem in the modern world. Even if the heavy metal ions are necessary for life, in higher concentrations they can be harmful to organisms and can cause serious health problems and can even lead to death. Since heavy metal ion poisoning due to the food chain is closely linked to the contamination of natural waters and soils, effective remediation is essential for health.

Mining activities influence natural water by using very large volumes of water in the process of ore processing and by water pollution from mine effluents and waste tailings. Increasingly, anthropogenic activities, such as mining, threaten the water sources we all depend on. Awareness of mining activities has increased lately. The price we pay for the daily use of minerals is often very high. Mining consumes, deviates and can seriously pollute water resources [1].

Drainage of mine water is achieved by drainage appropriate to the hydrological regime [1]. For mines with stable hydrological regime, groundwater evacuation is achieved through passive drainage, consisting of ordinary openings and exploitation mines (wells, galleries, inclined planes, rolling) [1]. For those with important aquifer formations and variable hydrological regime within wide limits, special drainage systems, consisting of pre-drilling works (drainage wells, boreholes, filters, dams, etc.) [1] may be applied. Mine waters can be reintroduced into the process stream in combination with clarified water from the tailings pond and/or recharge water collected from the surface source [1].

Dissolved elements such as:

- anions: SO_4^{2-}, HCO_3^-, PO_4^{3-}, Cl^-, Br^-;
- cations: Ca, Mg^{2+}, Cu^{2+}, Zn^{2+}, Fe^{3+}, Mn^{4+};
- microelements: As^{5+}, Zn^{2+}, Cd^{2+}, Ni^{2+}, Ti^{4+}, Be^{2+}, S^{2-}, V^{5+}, Co^{2+}, Ga^{3+}, Mo^{2+}, Ag^+, Sn^{4+}, Te^{4+}, Bi^{3+}, Ba^{2+} can be found in mine waters [1].

The heavy metals ions have serious effects on human health due to their acute and long term toxicity [2, 3]. They have the abilityto persist for a long time in natural ecosystems, and they also have the capacity to accumulate in successive levels of trophic chain determining the acute and chronic diseases [2].

The high acidity of acid mine drainage (AMD) has an indirect, but highly destructive effect [2]. Drainage water from the AMD becomes neutralized because of the precipitation of iron oxides and hydroxides that can deposit and imbed on the aquatic ecosystem bed determining cementation of substrates [2]. This will affect the small animals that use to feed the bottom of the aquatic

---

** email: claudiamaria_simonescu@yahoo.com* ecosystems that will be depleted [2]. This will affect the next trophic levels [2].

As environmental effects of acid mine waters became more visible over the years, a lot of remediation techniques have been developed.

Some of the processes used to remove these elements involve physical methods (e.g., membrane filtration, coagulation, stable and floating bed adsorption, reverse osmosis), chemical (such as neutralization with various materials including lime, ion exchange, adsorption, oxidation or chemical reduction) and biological processes [4]. The latter category presents some models that are not easy to implement under industrial conditions because they require high production costs and are too complex.

Published data has shown that adsorption on various solid materials is a preferred method, because it is simple, extremely selective, has a relatively low cost and presents very little to no problem [5-10]. Among the organic and inorganic materials used as heavy metal ion adsorbents can be mentioned: synthetic hydroxyapatite (HAP) and various composites containing polymers, zeolites, organic resins, sand, silicates, bentonite, carbon nanotubes, coal [11].

It has been reported that hydroxyapatite (HAP, $Ca_{10}(PO_4)_6(OH)_2$), a naturally occurring form of calcium phosphate and a strong tissue component can remove heavy metal ions from aqueous solutions due to its excellent reactivity and low solubility in water [12]. The high stability of the HAP structure together with its flexibility allows a wide variety of substitutions (especially Ca with divalent heavy metal ions such as Pb(II), Cu(II), Sb(III), Zn(II), Cd(II), Co(II), Ni(II), U(VI), Hg(II), As(V), of great importance in the field of environmental protection [13].

HAP can be synthesized by various methods, including sol-gel, wet precipitation, burning in the presence of microwaves and ultrasounds [14-21]. Its slightly alkaline pH and high biocompatibility will not cause any form of secondary environmental damage. The effectiveness of HAP in the removal of heavy metal ions depends to a large extent on the ionic nature, the charge, the diameter and the concentration, as well as the properties of the purified water (pH, temperature) [22]. In addition, the removal of HAP from the purified aqueous solution does not come without problems, as is the isolation of important heavy metals from it [23].

Thus, the main objectives of this research study are:

- synthesis of hydroxyapatite (HAP) samples using different synthesis conditions;
- characterization of hydroxyapatite samples (by the use of X-ray diffraction, FT-IR spectroscopy, specific surface measurements, Scanning Electron Microscopy (SEM));
- determining the influence of reaction conditions on the characteristics of HAP samples;
- use of hydroxyapatite samples in the process of retaining heavy metal ions from mine water samples;
- establishing the optimal conditions for the removal of heavy metal ions from mine waters.

Experimental part

Materials and equipments

The main raw materials used in the synthesis of hydroxyapatite samples are: calcium nitrate tetrahydrate ($Ca(NO_3)_2 \cdot 4H_2O$) (Merck origin), hydroorthophosphate ($(NH_3)_2HPO_4$ (Merck origin), 25% ammonium hydroxide (NH_4OH) (Merck orgin), sodium polyacrylate (Fluka) used as a surfactant.

Synthesized hydroxyapatite powders were characterized using modern analytical techniques such as X-ray diffraction, FT-IR analysis, specific surface determination, and Scanning Electron Microscopy (SEM).

X-ray diffraction was performed using an X-ray diffractometer, type D8 ADVANCE-GERMANY. The hydroxyapatite samples were studied on calcined samples at different temperatures. The X-ray diffractograms were recorded for 2Θ in the range 20-60° and then they were compared with those in the ASTM files (JCPDS, 09-0432).

FTIR spectra were recorded using a Fourier transformed spectrophotometer (Jasco FTIR 4100) using the KBr pellet method.

The specific surfaces (S_{BET}) of the hydroxyapatite samples were measured by adsorption-desorption of N_2 at -196 °C on an automatic adsorption system (Micromeritics ASAP 2020) using the Brunauer Emmett Teller method based on the partial pressure adsorption data (P/Po) in the range 0.05 - 0.3.

The size, morphology and shape of the HAP particles were studied by scanning electron microscopy (SEM), using a Carl Zeiss Auriga (Germany) scanning electron microscope.

Studies on the heavy metal ions retention from mine water were conducted with a GFL 3015 orbital shaker at a speed of 150 rpm.

The *p*H of the mine water sample and the *p*H of the treated water was determined using a Agilent 3200P laboratory pH meter.

A mine water sample was used as the waste water whose composition with respect to the metal ion content was determined by atomic absorption spectrometry using a ContrAA® 300 absorption spectrometer (Analytik Jena AG, Germany).

The chemical method in the solution was used to obtain the HAP nanoparticles. This requires an acid-base reaction that takes place at a solution *p*H value greater than 9 (to provide apatite structure formation) and reaction temperatures between 25 and 90 °C. Higher temperatures favor the formation of high crystallinity compounds. The precipitation method used involves precursors such as calcium nitrate and ammonium phosphate. Ammonia solution was used to maintain the *p*H constant throughout the reaction. Maintaining a certain degree of agitation throughout the reaction and the maturation process allows the compound to achieve the stoichiometry.

The variables that influence both the chemical balance and the purity and physical nature of the precipitate are: stoichiometry, concentration of solutions, temperature, the order of mixing, stirring time, *p*H,and agitation speed.

Preparation of hydroxyapatite was performed on the basis of the precipitation reaction from aqueous solutions under temperature and *p*H conditions, according to the reaction below:

$$10[Ca(NO_3)_2 \cdot 4H_2O] + 6(NH_4)H_2PO_4 + 14NH_4OH =$$
$$= Ca_{10}(PO_4)_6(OH)_2 + 20NH_4NO_3 + 52H_2O \qquad (1)$$

The two solutions were then mixed for 30 min, followed by continuous stirring for 30 and 60 min at room temperature respectively (mechanical stirrer was used). With the proper stirring, a homogeneous suspension with uniformly dispersed particles throughout the mass was sought, because by the manner in which this step is controlled depends ultimately on the size and the shape of the particle.

Filtration of the precursor was performed on a Buchner funnel to which a filter paper with pores smaller than the diameter of the precursor particles was attached. Drying

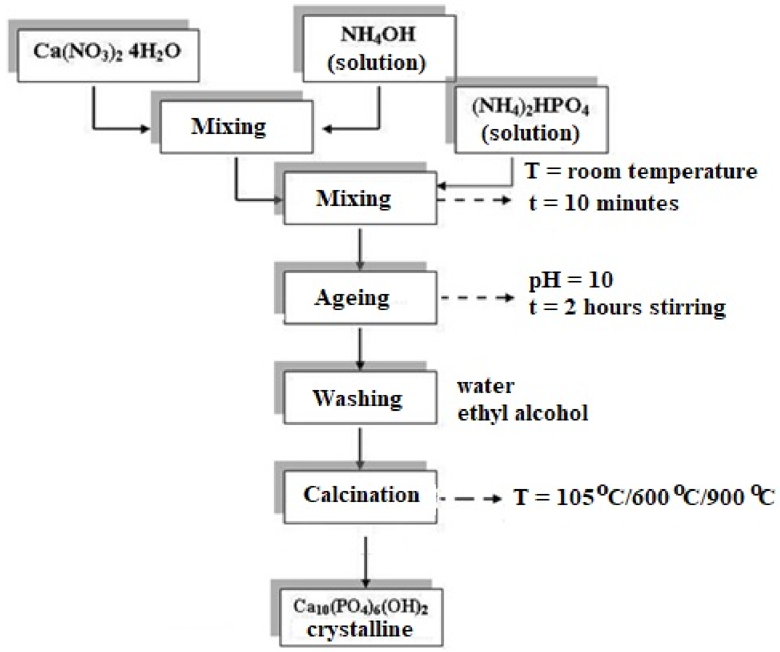

Fig.. 1. HAP obtaining by precipitation from aqueous solutions

of the precursor was carried out in the oven at 80 °C in order to remove the adsorbed water on the surface of the precipitate. The calcination was performed in a furnace with electric heating elements from SiC, (LEW), at different temperatures and different calcination times. The block diagram of hydroxyapatite preparation by precipitation from aqueous solutions is shown in Figure 1.

The main synthesis conditions and the raw materials used for the synthesis of hydroxyapatite samples are presented in Table 1.

As shown in Table 1, 6 hydroxyapatite samples were prepared from the same starting materials, but the calcination temperature was different. Samples oven-dried at 105 °C, but also samples which were calcined at 600 °C and 900 °C were prepared. The calcination time was 2 hours. Sodium polyacrylate was used as surfactant to prevent aggregation of HAP nanoparticles.

HAP samples characterization

Characterization of synthesized hydroxyapatite powders was performed using modern techniques such as X-ray diffraction, FT-IR analysis, specific surface determination and Scanning Electron Microscopy (SEM).

X-ray diffraction spectra were recorded using an X-ray diffractometer, D8 ADVANCE-GERMANY type the diffractograms recorded for 2Θ in the 20-60^o range were compared with those in the ASTM files (JCPDS: 00-009-0432) [24].

The X-ray diffraction spectra of non-calcined and calcined hydroxyapatite samples are shown in figures 2-7.

As it can be seen from these figures, all X-ray diffraction spectra of synthesized HAP samples present diffraction peaks characteristic of hydroxyapatite indexed according to the JCPDF: 00-009-0432 (Joint Committee on Powder Diffraction File) database [24]. No other diffraction peaks were found, so it can be concluded that the synthesized HAP samples do not present impurities as the only crystalline HAP phase being identified in the samples.

It can be seen that the spectra of non-calcined powders exhibit wider diffraction peaks indicating that the respective powders are less crystalline (have lower crystallinity). The spectra of calcined powder samples show sharper diffraction peaks indicating well-crystallized

Table 1
RAW MATERIALS AND CONDITIONS FOR THE SYNTHESIS OF HYDROXYAPATITE SAMPLES

No.	Sample code	Materii prime	Condiții de reacție
1	**HAP-1-U**	$Ca(NO_3)_2\cdot 4H_2O$ (calcium nitrate tetrahydrate) $[(NH_3)_2HPO_4$ (diammonium hydro-orthophosphate) NH_4OH	precipitation at room temperature pH = 10; reaction time 2 hours final washing with ethanol **drying in oven at 105 °C**
2	**HAP-1-600**	$Ca(NO_3)_2\cdot 4H_2O$ (calcium nitrate tetrahydrate) $[(NH_3)_2HPO_4$ (diammonium hydro-orthophosphate) NH_4OH	precipitation at room temperature pH = 10; reaction time 2 hours final washing with ethanol **calcination at 600 °C (2 hours)**
3	**HAP-1-900**	$Ca(NO_3)_2\cdot 4H_2O$ (calcium nitrate tetrahydrate) $[(NH_3)_2HPO_4$ (diammonium hydro-orthophosphate) NH_4OH	precipitation at room temperature pH = 10; reaction time 2 hours final washing with ethanol **calcination at 900 °C (2 hours)**
4	**HAP-2-U**	$Ca(NO_3)_2\cdot 4H_2O$ (calcium nitrate tetrahydrate) $[(NH_3)_2HPO_4$ (diammonium hydro-orthophosphate) NH_4OH Surfactant: Na-PAA (sodium polyacrylate), 1% weight;	precipitation at room temperature pH = 10; reaction time 2 hours final washing with ethanol **drying in oven at 105 °C**
5	**HAP-2-600**	$Ca(NO_3)_2\cdot 4H_2O$ (calcium nitrate tetrahydrate) $[(NH_3)_2HPO_4$ (diammonium hydro-orthophosphate) NH_4OH Surfactant: Na-PAA (sodium polyacrylate), 1% weight;	precipitation at room temperature pH = 10; reaction time 2 hours final washing with ethanol **calcination at 600 °C (2 hours)**
6	**HAP-2-900**	$Ca(NO_3)_2\cdot 4H_2O$ (calcium nitrate tetrahydrate) $[(NH_3)_2HPO_4$ (diammonium hydro-orthophosphate) NH_4OH Surfactant: Na-PAA (sodium polyacrylate), 1%weight;	precipitation at room temperature pH = 10; reaction time 2 hours final washing with ethanol **calcination at 900 °C (2 hours)**

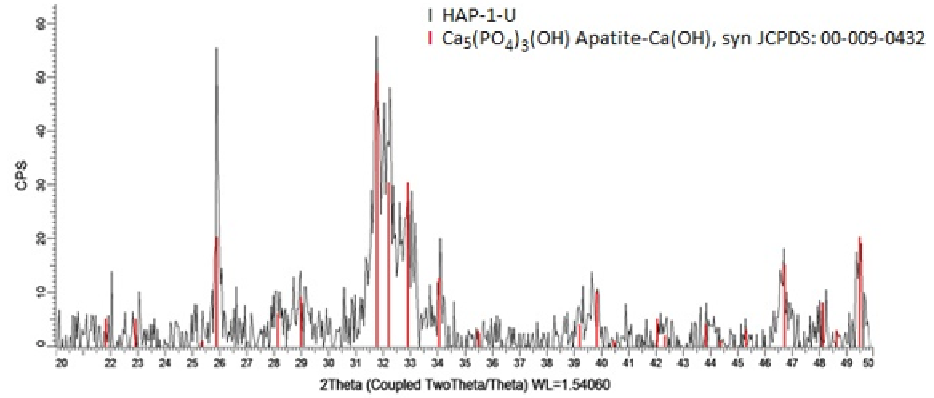

Fig.2. X-ray diffraction spectrum of the HAP-1-U sample

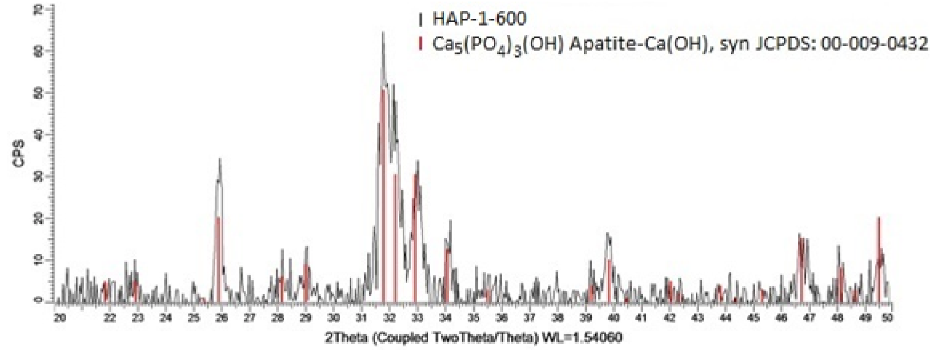

Fig.3. X-ray diffraction spectrum of the HAP-1-600 sample

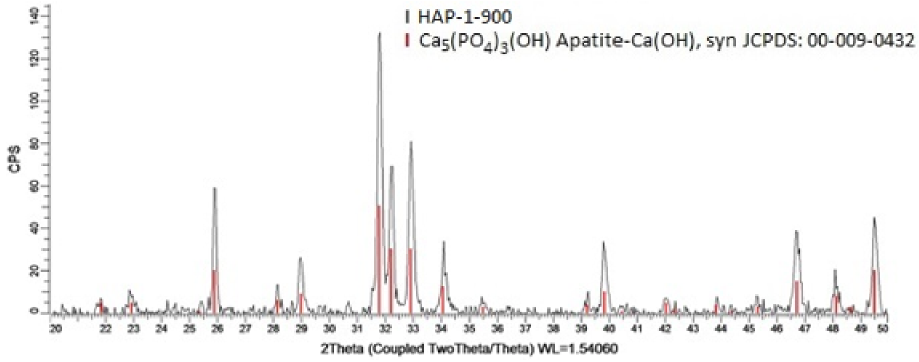

Fig.4. X-ray diffraction spectrum of the HAP-1-900 sample

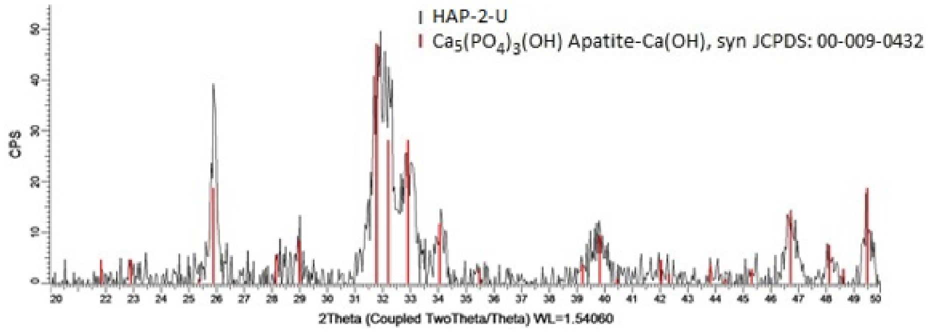

Fig.5. X-ray diffraction spectrum of the HAP-2-U sample

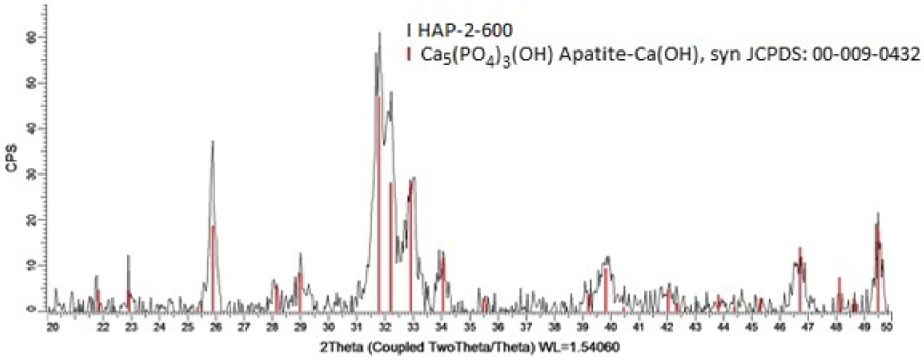

Fig.6. X-ray diffraction spectrum of the HAP-2-600 sample

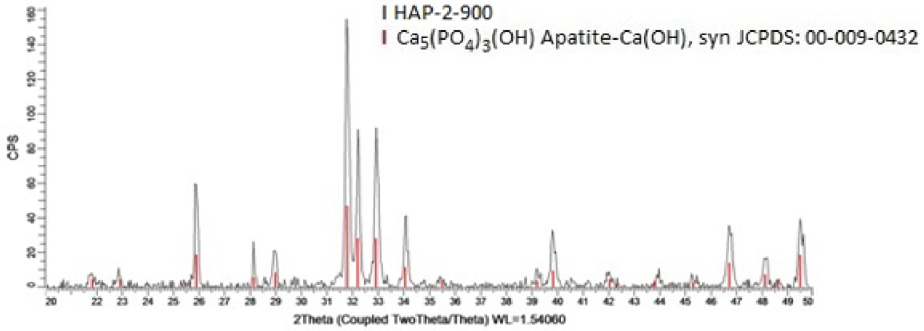

Fig.7. X-ray diffraction spectrum of the HAP-2-900 sample

phases (crystallinity increases with the increase of calcination temperature).

Elementary cell parameters were calculated by processing the diffractograms using the most representative peaks. The average particle diameter was calculated using the Scherrer equation:

$$t = 0.9/(B^2_M-B^2_S) \times \cos\Theta \qquad (1)$$

where:

t = particle diameter,

λ = wavelenght for K line,

B_M = the width of the diffraction line, measured at half height of the maximum intensity,

Sample	D (Å)
HAP-1-U	661.9
HAP-1-600	301.9
HAP-1-900	523.6
HAP-2-U	610.3
HAP-2-600	382.8
HAP-2-900	552.3

Table 2
THE AVERAGE DIAMETER VALUES OF THE HYDROXYAPATITE PARTICLES DETERMINED FROM THE X-RAY DIFFRACTION SPECTRA

B_S= the width of the diffraction line, measured at half height of the maximum intensity for standard sample,

Θ= Bragg's angle.

The values of average particle diameter calculated by the use of Scerrer's equation are shown in table 2.

From the analysis of the data presented in Table 2 it can be seen that non-calcinated hydroxyapatite samples have a higher average particle diameter compared to the calcined hydroxyapatite samples. Another observation is that for the calcined samples the increase of the calcination temperature results in an increase in the average diameter of the nanoparticles which will result in a decrease of the specific surface.

Lower average particle diameter values were observed for the HAP-2 samples using surfactant. On the other hand, the method of hydroxyapatite preparation by solid phase reaction allows the obtaining of stoichiometric compounds with high degree of crystallinity (due to high calcination temperatures) and low average particle diameter values.

Infrared Spectroscopy (FTIR) allows the analysis of material characteristics, being a complementary technique to X-ray diffraction (DRX) measurements, by identification of the main functional groups present in the structure of the analyzed materials. The FT-IR spectra were recorded in the range of 40 ÷ 4000 cm^{-1}.

Spectrophotometric measurements are complement to those of X-ray diffraction. These besides qualitative phase identification also highlight the ionic species (the groups characteristic of the HAP compound) presented in compounds.

The main FT-IR peaks and their assignments are presented in Table 3.

The FT-IR spectra of all the HAP samples show only peaks characteristics to the PO_4^{3-} and water molecules adsorbed [25]. tThere is no evidence of the presence of CO_3^{2-}impurification because there are no peaks at the wavelengths at 875 and 1469 cm^{-1}. The spectra are similar for all synthesized HAP samples.

Peak (cm^{-1})	Assignment
3573-3574	$\nu_{(OH)}$ (O-H stretching vibration)
1090	ν_3 vibration mode of the PO_4^{3-} group
965	ν_1 nondegenerated symmetric stretching mode of the P-O bond
631	ν_4 vibration mode of the PO_4^{3-} group
472	ν_2 vibration mode of the PO_4^{3-} group

Table 3
THE FT-IR PEAK ASSIGNMENTS

Nitrogen sorption isotherms at -196 ° C were recorded on a Micromeritics ASAP 2020 automated gas sorption system. The samples were degassed at 200 °C for 4 h under vacuum prior to N_2 uptake. The specific surfaces (S_{BET}) were calculated according to the Brunauer-Emmet-Teller (BET) equation using absorption data in the relative pressure range between 0.05 and 0.30. The specific surface values characteristic of the synthesized samples are shown in Table 4.

HAP Sample	S_{BET} (m^2/g)
HAP-1-U	69.8
HAP-1-600	35.,5
HAP-1-900	10.9
HAP-2-U	76.4
HAP-2-600	41.3
HAP-2-900	10

Table 4
THE SPECIFIC SURFACES (S_{BET}) VALUES FOR HAP SAMPLES

From the analysis of the data on the specific surface, the following conclusions can be drawn:

- the highest value of the specific area was registered for non-calcinated HAP samples;
- calcination has as effect a secrease in the value of the specific surface;
- the increase of calcination temperature causes a more pronounced decrease of the specific surface value;
- a 7-fold decrease in the specific surface area was determined by calcination at 900 °C;
- the addition of surfactant (dispersant) has resulted in an increase in the specific surface area, which will result in an increase in the retention capacity of heavy metal ions in wastewater.

The scanning electron microscope (SEM) was used for the morphological study of nanoparticles of hydroxyapatite. Figures 8-10 shows the SEM images of the as-prepared hydroxyapatite nanoparticles, still used as synthetic adsorbents. Therefore, the size, the shape and the typical pore structure of the synthesized n-HAP samples are further observed.

Figure 8 shows the SEM images of the as-prepared hydroxyapatite nanoparticles.

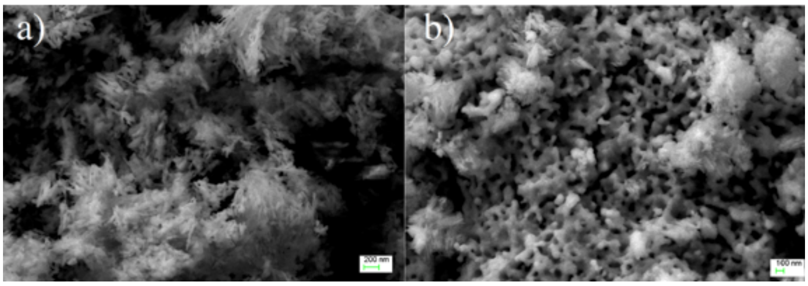

Fig.8. SEM images of HAP samples: a) HAP-1-U; b) HAP-2-U, (magnification 50.00 K X)

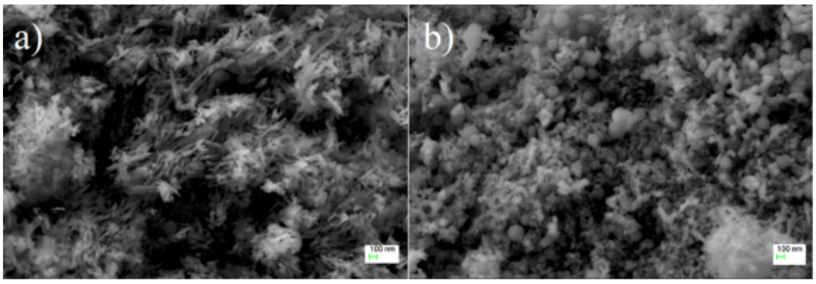

Fig.9. SEM images of HAP samples: a) HAP-1-600, b) HAP-2-600, (magnification 50.00 K X)

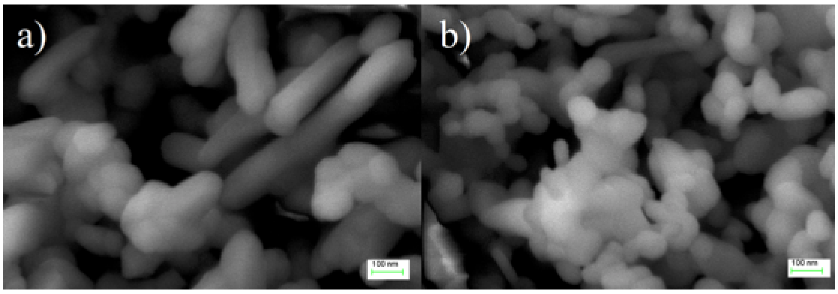

Fig.10. SEM images of HAP samples: a) HAP-1-900; b) HAP-2-900, (magnification 200.00 K X)

The hydroxyapatite nanoparticles formed without surfactant were highly agglomerated, presents a uniform needle-like shape, and these nanocrystals are presented in agglomerates of few microns (fig. 8a).

SEM images show the effects of surfactants on the particle size and their morphology nanoparticles; by comparing, it can be seen that by adding 1% surfactant the size of the HAP-2 nanoparticles decreases from 66 to 61 nm. Moreover, it also yields the combination of the small nanorods with micrometric spheric-like structures (agglomerates of 1-2μm), fig. 8b.

Figure 9 depicts SEM photographs of the two HAP nanopowders thermal treated at 600^{o}C.

The particle size of HAP-2 sample (a lot of them with spherical morphology, with average diameter of in the range 75-100nm (Fig. 9a) with a tendency of agglomerating, whereas the particle size of HAP-1 consisting of elongated particles of average diameter of 15-20nm and 150-200nm in length, constituted in filiform structures (Fig. 9b). Fig 9b also confirms that the nanoparticles are spherical in nature. The average size of the nanoparticle estimated from the SEM images are in good agreement with that calculated from that of XRD.

Figure 10 presents SEM photographs of the HAP nanopowders, after sintering at 900^{o}C.

The samples obtained after heat-treatment at the sintering temperature (900 ^{o}C), exhibit very well defined elongated and compact nanorods, constituting agglomerates of dimensions of about 400nm (fig. 10a), The samples obtained after sintering at 900^{o}C, with addition of surfactant, exhibit mainly agglomerates of rounded particles (with superficial melting aspect), with the size of 100-350nm (fig. 10b). For both the samples, the particles appeared to be bound together into agglomerates of various sizes which strongly depend on the sintering temperature. For the samples treated at 900^{o}C, no individual particles could be observed.

In conclusion, the addition of surfactant allowed to obtain nanoparticles of HAP with spherical morphology (smaller particle size but higher specific surface area) with better adsorbent qualities, as will be demonstrating by the heavy metals retention tests from aqueous solutions.

Results revealed that the morphology and size of HAP nanoparticles can be effectively controlled by the presence of surfactant. In addition, the temperature of the treatment (calcination and finally, sintering) plays an important role in controlling the morphology and size of HAP particles as potentially used as adsorbents.

Surfactant can also be used in order to prevent nanoparticle agglomeration in the solution, and also to obtained spherical particles. To examine the influence of surfactants on morphology and size of HAP particles, the synthesis process was conducted with and without surfactant addition. Sintering temperature has a major effect on the morphology, size and chemical composition of the product. During the heat treatments, because the phenomenon of sintering, the particles grow from nano to microscale. Moreover, it also yields the combination of the nanorods with micrometric spherical-like structures. However, the composition, physicochemical properties (crystal size and morphology of synthetic apatites) are extremely sensitive to preparation conditions.

Remediation studies

The six hydroxyapatite samples were used in the process of removing metallic ions from mine water. In order to determine the optimal conditions for the removal of metal ions, batch tests were carried out using samples of 0.05 g of HAP and 50 mL of wastewater. Tests were performed at different times (in the range 5 minutes - 720 minutes) and room temperature on a GFL 3015 orbital shaker at 150 rpm.

The amount of metal ions retained on nanoparticles of hydroxyapatite was calculated as the difference between the concentration of metal ions in the initial mine water and the concentration of metal ions present in the solution

Table 5
CHARACTERISTICS OF MINE WATER USED IN THE REMEDIATION PROCESS

Wastewater	pH	Mn(II), mg/L	Fe(III), mg/L	Zn(II), mg/L	Pb(II), mg/L	Ni(II), mg/L
Mine water	2.6	773.25	437.9	45.8	4.68	1.97

after reaching the equilibrium (or at various contact times) (equation 2).

$$Q=\frac{(C_i-C_f)V}{m}, \qquad (2)$$

where: Q(mg/g) -quantity of heavy metal ions retained on adsorbent;

C_i (mg/L) -the concentration of metal ions in mine water;

C_f (mg/L) -the final concentration of the metal ions in the solution at different times after adsorption;

V(L) -mine water volume;

m(g) -nano-HAP quantity (g).

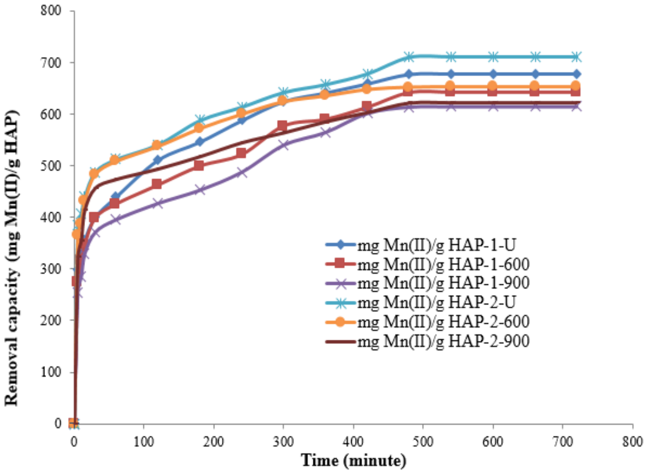

Fig.11. Effect of contact time on the hydroxyapatite samples capacity to retain Mn(II) ions from mine water

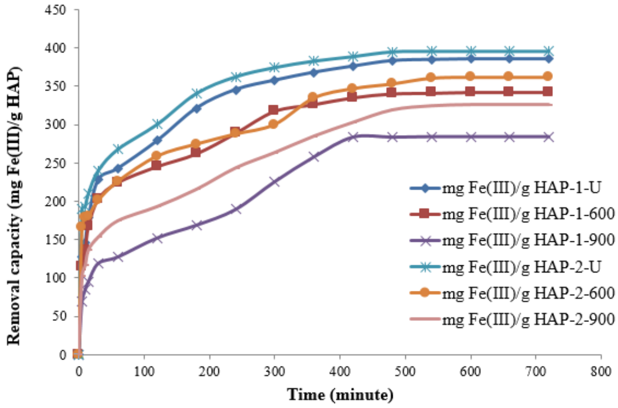

Fig.12. Effect of contact time on the hydroxyapatite samples capacity to retain Fe(III) ions from mine water

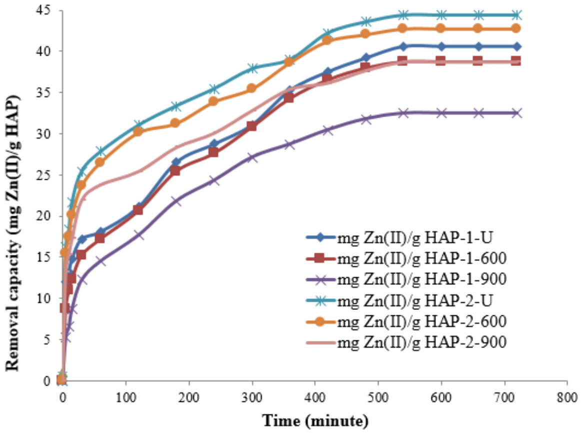

Fig.13. Effect of contact time on the hydroxyapatite samples capacity to retain Zn(II) ions from mine water

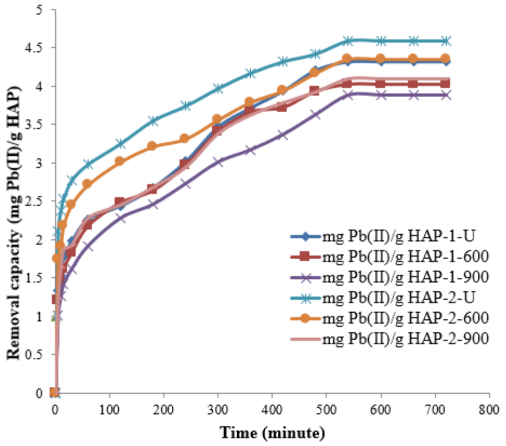

Fig.14. Effect of contact time on the hydroxyapatite samples capacity to retain Pb(II) ions from mine water

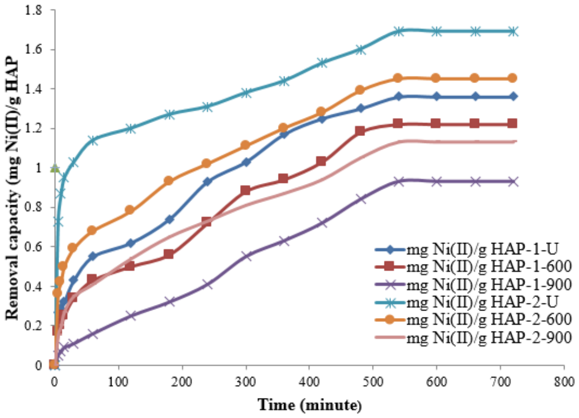

Fig.15. Effect of contact time on the hydroxyapatite samples capacity to retain Ni(II) ions from mine water

The mine water used in this experimental study has the following characteristics (Table 5).

The results obtained with regard to the effect of the contact time are shown in the figures below.

The data presented in figures 11-15 reveals the followings:

- the amount of metal ions retained on the HAP varies according to the value of the contact time between the two phases;
- initially (in the first 60 min) the process of metal ion retention on HAP is a rapid process due to the large number of free active centers that will be occupied by metal ions in mine water;
- the time required to achieve the equilibrium is, for all 6 HAP samples tested, approximately 9-10 h (this being called the equilibrium time or the optimal time for the remediation process);
- for both HAP sets samples, a variation of heavy metal ions retention capacity in the series: HAP-1/2-U > HAP-1/2-600 > HAP-1/2T-900; this variation in the retention capacity is consistent with the variation of the specific surface;
- compared to the two sets of HAP samples, the following variation of the HAP-2-U> HAP-1-U retention capacity is found - this variation is also due to the variation of the specific surface. In this case, the addition of surfactant resulted in an increase in the specific surface (in the case of HAP-2-symbolized samples) with effect on the retention capacity (an increase in the retention capacity);

- the values of the retention capacity differ depending on the nature of the metal ion: $Q_{Mn(II)} > Q_{Fe(III)} > Q_{Zn(II)} > Q_{Pb(II)} > Q_{Ni(II)}$.

The second parameter analyzed was the amount of adsorbent (HAP). Different amounts of HAP (in the range 0.01 - 0.075g) were used in this set of experiments. The contact time between mine water and HAP samples was 10 h. The experiments were performed at room temperature and 150 rpm using a 50 mL volume of wastewater.

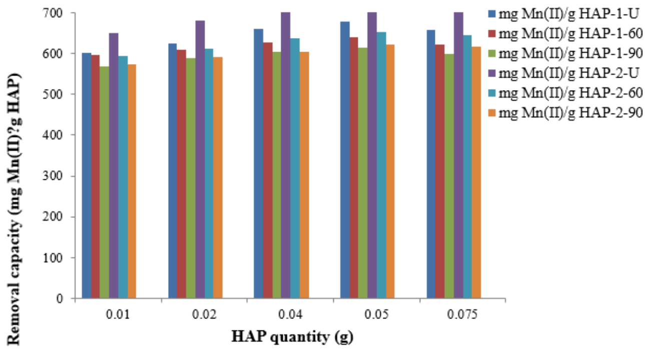

Fig.16. The effect of hydroxyapatite samples quantity on Mn(II) adsorption capacity from mine wastewater

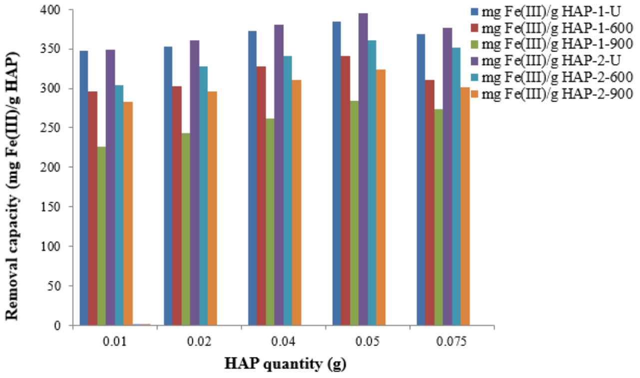

Fig.17. The effect of hydroxyapatite samples quantity on Fe(III) adsorption capacity from mine wastewater

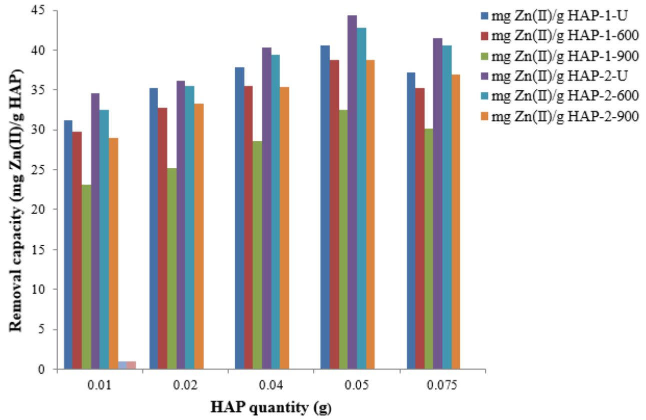

Fig.18. The effect of hydroxyapatite samples quantity on Zn(II) adsorption capacity from mine wastewater

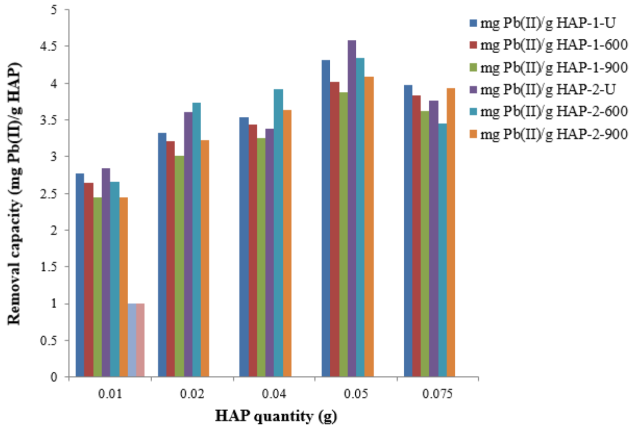

Fig.19. The effect of hydroxyapatite samples quantity on Pb(II) adsorption capacityfrom mine wastewater

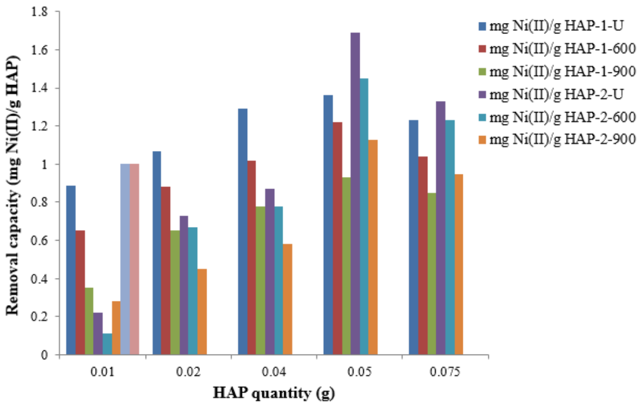

Fig.20. The effect of hydroxyapatite samples quantity on Ni(II) adsorption capacity from mine wastewater

The experimental results are shown in Figures 16-20.

As can be seen from the analysis of the experimental results presented in Figures 16-20 for all the metal ions retained in the mine water, an increase in the retention capacity was found with increasing the amount of adsorbent used up to a certain amount (optimum quantity) after which a slight decrease in retention rate has been observed. In this case the optimal amount of experimentally determined adsorbent was 50 mg.

The variation of the retention capacity is according to the variation of the specific surface and the morphological properties of the HAP samples prepared.

The *p*H of the purified water after the remediation process was measured and an increase from 2.6 to 5.5 was found. This increase in *p*H indicates that the metal ion retention mechanism occurs through chemical reactions.

Conclusions

Experiments have been carried out on the synthesis, characterization and application of hydroxyapatite samples in wastewater treatment processes in the mining industry. In the synthesis of hydroxyapatite powders, the influence of the calcination temperature and the presence of a surfactant/dispersant on the adsorbant properties of the HAP powders was followed.

It has been found that the calcination temperature has the effect of increasing crystallinity. Non-calcinated powders are less crystalline (have lower crystallinity) and the calcined ones are well crystalline (higher crystallinity as the calcination temperature is higher).

Non-calcinated hydroxyapatite powders have a larger average particle diameter compared to calcined hydroxyapatite samples. Another observation is that for calcined samples, the increase in calcination temperature results in an increase in the average diameter of nanoparticles, which will result in a decrease in the specific surface area.

In the case of samples synthesized in the presence of the surfactant, lower average particle diameter values were observed.

As a result, the method of forming hydroxyapatite by solid phase reaction allows the obtaining of stoichiometric compounds with high degree of crystallinity (due to high calcination temperatures) and low average particle diameter values.

Analyzing the results obtained in the process of remediation of the waste water from the mining industry, the following conclusions can be drawn:

- in the experiments on the influence of contact time it was found that in the first 60 minutes the process of metal ion retention on HAP is a rapid process because of the large number of free active centers presented on adsorbent's surface;

- the equilibrium time for all 6 samples of HAP tested was approximately 9-10 hours;

- for both HAP sets, a variation of heavy metal ions retention capacity in the series: HAP-1/2-U > HAP-1/2-600 > HAP-1/2-900; this variation in the retention capacity is consistent with the variation of the specific surface;

- by comparing the two sets of HAP samples, the following variation of the HAP-2-U> HAP-1-U retention capacity was found - this variation is also due to the variation of the specific surface.

- the addition of surfactant resulted in an increase in the specific surface area (in the case of HAP-2-symbolized samples) with effect on retention capacity (an increase in retention capacity);

- the values of the retention capacity differ depending on the nature of the metal ion: $Q_{Mn(II)} > Q_{Fe(III)} > Q_{Zn(II)} > Q_{Pb(II)} > Q_{Ni(II)}$.

- the optimal amount of adsorbent needed to solve a volume of 50 mL of wastewater in the mining industry is 0.05 g.

- the *p*H change of mine water of 2.6 to 5.5 indicates that the metal ion retention mechanism occurs through chemical reactions.

The metal ions retention capacity recommends application of hydroxyapatite adsorbents in the process of remediation of mining wastewater.

References

1.FODOR, D., Buletinul Agir no. 3, 2006, p.2.

2.SIMATE, G.S., NDLOVU, S., J. Environ Chem. Eng. 2, 2014, p. 1785.

3.SIMONESCU, C.M., TANASE, I.-R., PURCARU, I.N., TARDEI, C., MARINESCU, V., Rev. Chim (Bucharest) **70**, no. 5, 2019, p 1758.

4.CULITA, D.-C., SIMONESCU, C.M., PATESCU, R.-E., STANICA, N., Rev.Chim (Bucharest) **69**, no. 9, 2018, p. 2323.

5.BUSUIOC, T.L., SIMONESCU, C.M., NECHIFOR, G., RADOI, E., GIRBEA, I.E., Rev. Chim.(Bucharest) **69**, no.6, 2018, p 1293.

6.DELEANU, C., SIMONESCU, C. M., CONSTANTINESCU, I., Rev. Chim.(Bucharest) **59**, no 6, 2008, p. 639.

7.SIMONESCU, C.M., DINCA, O.-R., OPREA O., CAPATINA, C., Rev. Chim.(Bucharest) **62**, no. 2, 2011, p. 183.

8.SIMONESCU C.M., MARIN, I., TARDEI, CH., DRAGNE, M., CAPATINA, C., Rev. Chim.(Bucharest) **65**, no. 7, 2014, p. 750.

9.SIMONESCU C.M., DELEANU C., STANCU M., CAPATINA, C., Journal of Environmental Protection and Ecology **13**, no. 2, 2012, p. 462.

10.MELINESCU A., TARDEI, C., SIMONESCU C.M., MARINESCU, V., MICLEA, A., Romanian Journal of Materials, (Rev. Rom. Mater.) **43**, no. 2, 2013, p. 223.

11.PATESCU R.-E., SIMONESCU C.M., NECHIFOR, G., TARDEI, C., IONASCU, C.I., Rev.Chim. (Bucharest) **69**, no.4, 2018, p. 759.

12.PATESCU, R.-E., SIMONESCU, C.M., BUSUIOC, L.T., ONOSE, C., MELINESCU, A., Rev. Chim. (Bucharest)**67**,no.10, 2016, p. 1899.

13.TARDEI, C., SIMONESCU, C.M., ONOSE, C., SAVA, B.A., BOROICA, L., SBÂRCEA, B.-G., Romanian Journal of Materials, **46**, no. 3, 2016, p. 289.

14.SIMONESCU C.M., PATESCU, R.-E., BUSUIOC, L.T., ONOSE, C., MELINESCU, A., LILEA, V., Rev. Chim. (Bucharest) **67**, no.8, 2016, 1498.

15.SABU, U., LOGESH, G., RASHAD, M., JOY, A., BALASUBRAMANIAN, M., Ceram. Int. **45**, no. 6, 2019, p. 6718.

16.TRAKOOLWANNACHAI, V., KHEOLAMAI, P., UMMARTYOTIN, S., Composites Part B **173**, 2019, 106974.

17.AI, F., YAN, J., RUAN, H., ZOU, J., CHI, W., CAO, C., LI, W., ZHOU, K., Ceram. Int. **45**, 2019, p. 16399.

18.VAHDAT, A., GHASEMI, B., YOUSEFPOUR, M., Environ. Nanotechnol, Monit. Manag. **12**, 2019, 100233.

19.KAKIAGE, M., ODA, S., Mater. Letter **248**, 2019, p. 114.

20.MOHD PU'AD, N.A.S., KOSHY, P., ABDULLAH, H.Z., IDRIS, M.I., LEE, T.C., Heliyon **5**, 2019, e01588

21.HAJIMIRZAEE, S., CHANSAI, S., HARDACRE, C., BANKS, C.E., DOYLE, A.M., J.Solid State Chem. **276**, 2019, p. 345.

22.SAVA, B.A., TARDEI, C., SIMONESCU, C.M., BOROICA, L., MELINESCU, A., Optoelectronics and Advanced Materials – Rapid Communications **9**, no. 11-12, 2015, p. 1415.

23.SIMONESCU C.M., TATARUS, A., TARDEI, C., PATROI, D., DRAGNE, M., CULITÃ, D.C., PÃTESCU, R.-E., BUSUIOC, L.T., MELINTE, I., Rev. Chim. (Bucharest) **66**, no.5, 2015, p 732.

24.BOUJAADY, H.EL, MOURABET, M., ABDELHADI, EL.R., BENNANI-ZIATNI, M., EL HAMRI, R., ABDERRAHIM, T., Mater. Environ. Sci. **7**, no. 11, 2016, p. 4049.

25.POPA, C.L., ALBU, M., BARTHA, C., COSTESCU, A., LUCULESCU, C., TRUSCA, R., ANTOHE, S., Romanian Reports in Physics, **68**, no. 3, 2016, p. 1149.

Manuscript received: 5.07.2019